Upper Stark State Collisional Relaxation Cross Sections for Single Rotational States of CH_3F

C. Vallance, W-P. Hu, and P. W. Harland*

Department of Chemistry, University of Canterbury, Christchurch, New Zealand

Received: September 10, 1998; In Final Form: November 16, 1998

A radiofrequency electric resonance cell has been used to modulate individual rotational states present in a state-selected molecular beam of symmetric top molecules prepared for use in a beam attenuation experiment. Tagging states in this way allows cross sections for collisionally induced ΔM transitions to be measured for single rotational states. A hexapole transmission curve attenuation method reported earlier suffered from poor rotational state resolution and the measurement of cross sections was very time consuming in comparison to the method reported here. Cross sections measured using the two different methods show remarkably good agreement.

1. Introduction

Measurements of state-resolved rotationally inelastic collision cross sections were carried out on diatomic molecules in the early 1960s. Toennies[1−4] used a quadrupole electrostatic filter to prepare a rotationally state selected beam of TlF, which was then focused into a gas-filled collision chamber. A second quadrupole filter placed slightly off axis was used to analyze the state distribution of the scattered beam molecules. Cross sections for ΔJ transitions were measured for a variety of scattering gases and were found to be highly dependent on the scattering species. Total collisional attenuation cross sections for the $J = 2$ rotational state of TlF ranged from 152 Å^2 using He as the scattering gas, to 2140 Å^2 using NH_3. In a later study,[5,6] crossed molecular beams were used to investigate the inelastic collision cross sections of CsF seeded in Xe with a range of scatterers, including the inert gases, N_2, CO_2, CH_4, and SF_6, and symmetric top alkyl halides. The use of crossed beams greatly improved the resolution by narrowing the velocity distribution of the scattering gas relative to the "bulb" type experiment. Cross sections reported for ($\Delta J = 1, 2$; $\Delta M = 0, 1$) transitions ranged from 0.5 to 620 Å^2 depending on the particular transition and also on the scattering gas.

Blunt et al.[7] have recently published collisional attenuation cross sections for neat and seeded beams of CH_3Cl with a range of scatterers. A hexapole electrostatic filter was used for state selection and the hexapole chamber itself was pressurized for the attenuation experiments. Cross sections were found to lie in the range from 200 Å^2 for neat CH_3Cl on Ne to 670 Å^2 for a beam of 5% CH_3Cl in Xe on N_2. Collision cross sections of CH_3F with various scattering gases were also measured.[8]

Wiediger et al.[9] have recently shown that molecular beam radiofrequency electric resonance spectroscopy is a highly useful technique for interrogating the rotational states present in a molecular beam of oriented symmetric top molecules. It was also suggested that the technique might prove useful for labeling individual rotational states in studies of the orientation dependence of collision processes. The current work utilizes this suggestion in determining collisional attenuation cross sections for rotationally state selected beams of seeded CH_3F. Cross sections with a range of scattering gases have been measured for the $|11\rangle$, $|21\rangle$, and $|31\rangle$ $|JK\rangle$ states of CH_3F.

2. Theory

2.1. Rotationally State Selected Molecular Beams. When a symmetric top molecule enters a hexapole electric field it experiences a radial force which depends on its rotational quantum state $|JKM\rangle$. Solving the appropriate equations of motion shows that there are three cases to consider: $KM > 0$, $KM < 0$, and $KM = 0$. A lower Stark state molecule with $KM > 0$ has its dipole aligned with the electric field vector and follows divergent trajectories within the hexapole, resulting in its loss from the beam. In contrast, a molecule in an upper Stark state ($KM < 0$) follows a sinusoidal trajectory through the hexapole field and focuses on the axis at a point along its trajectory which is dependent on the high voltage applied to the hexapole rods. This focusing forms the basis for rotational state selection of symmetric top molecular beams using a hexapole; the high voltage can be swept to successively bring different rotational states into focus. States with $KM = 0$ are not affected by the hexapole field and follow linear trajectories through the hexapole region.

2.2. Radiofrequency Resonance Spectroscopy. In order to carry out a resonance experiment the hexapole field is split into two sections, known as the A and B fields, and a resonance or C field is introduced between them. The resonance field consists of perpendicular components of RF and DC radiation and excites rotational transitions between the upper Stark state symmetric top molecules which survive trajectories through the A field. A resonance field consisting of crossed RF and DC fields is required in order for a transition to occur; there must be some component of the excitation radiation along the transition dipole of the molecule. For a symmetric top molecule the transition dipole is orthogonal to the molecular axis, requiring that the RF radiation which excites the ΔM transitions must have a component at right angles to the DC field along which the molecular axes align.

A rotational state of a symmetric top molecule with quantum numbers $|JKM\rangle$ in an electric field has a first-order Stark energy given by

$$W = -\mu E \frac{KM}{J(J+1)} \tag{1}$$

10.1021/jp983671g CCC: $18.00
Published on Web 01/26/1999

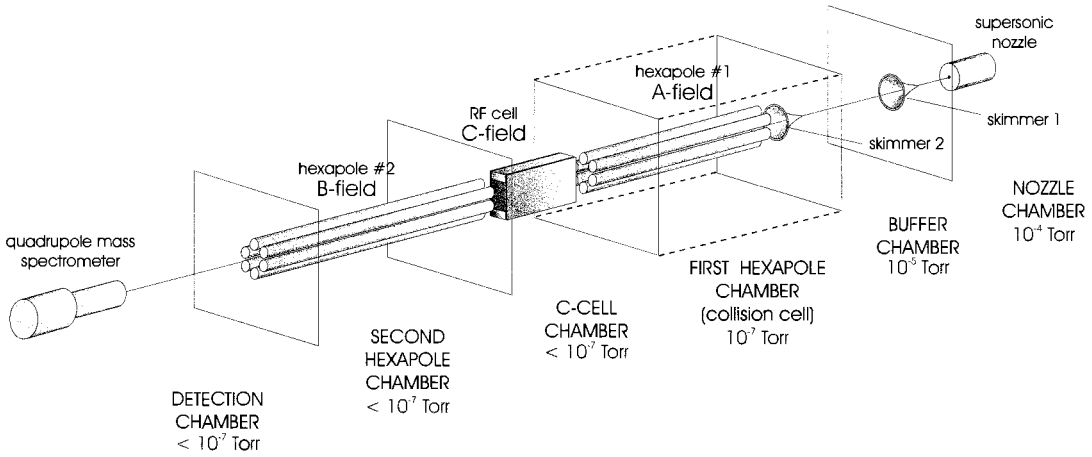

Figure 1. Schematic of the experimental arrangement used for measuring collisional attenuation cross sections (hexapole exit apertures and collision cell partitions not shown).

where μ is the permanent molecular dipole moment and E is the electric field strength. The spectroscopic selection rules for symmetric top molecules in an inhomogeneous electric field are given below (2), although Oka[10,11] and Phillips[12] have suggested that $\Delta M > \pm 1$ transitions are possible under some circumstances.

$$\Delta J = 0, \pm 1; \quad \Delta K = 0; \quad \Delta M = 0, \pm 1 \tag{2}$$

In the experiments reported here, the beam is irradiated with RF tuned to specific $\Delta M = \pm 1$ transitions; $\Delta J = 0$ and the energy of a transition is given by

$$\Delta W = -\mu E \frac{KM}{J(J+1)}[M - (M \pm 1)] \tag{3}$$

$$= \pm \mu E \frac{K}{J(J+1)} \tag{4}$$

In order to excite a transition the frequency of the microwave radiation must satisfy $h\nu = \Delta W$, so that

$$\frac{\mu E}{h\nu} = \frac{J(J+1)}{K} \tag{5}$$

Equation 5 shows that a spectrum of the $|JK\rangle$ states in a molecular beam may be obtained by sweeping either the DC field strength E or the RF frequency ν, while the other is held constant. For example, as a particular rotational state with $M = -1$ in the upper Stark state selected molecular beam passing through the C field comes into resonance, stimulated emission occurs, converting a small fraction of upper Stark state molecules to the $M = 0$ state via a ΔM transition. Since molecules which have undergone such a transition no longer focus in the second hexapole the beam intensity is reduced relative to the non-resonance condition. During an experiment the RF is square wave modulated and the small difference signal ($S_{\mathrm{RFoff}} - S_{\mathrm{RFon}}$) measured at the mass spectrometer is detected using a phase sensitive lock-in amplifier, which is essentially a narrow bandpass filter tuned to the frequency of the signal. If the RF and DC are tuned to the values at which a particular state comes into resonance, the modulation in the signal corresponding to that state effectively labels it, allowing it to be detected separately from the other rotational components of the beam.

2.3. Collision Cross Sections. The cross section obtained in a beam attenuation experiment is determined from measured quantities using Beer's law

$$\ln\frac{I_0}{I} = n\sigma l = \frac{\sigma l P}{k_{\mathrm{B}}T} \tag{6}$$

in which I and I_0 are the transmitted and incident beam intensities, n is the particle number density in the collision region, l is the path length through the collision region, σ is the cross section, P is the pressure in the collision region, k_{B} is Boltzmann's constant, and T is the temperature of the collision gas.

In the current experiments the A field region is pressurized, defining the geometric path length as the distance from the second skimmer to the exit aperture of the first hexapole, 0.548 m.

3. Experimental Section

A schematic of the experimental arrangement is shown in Figure 1. The supersonic nozzle used in this work consists of a small cylindrical copper chamber fitted with a 70 μm molybdenum aperture. Typical nozzle stagnation pressures are around 100 Torr, limited by the pumping capacity of the 10 in. VHS-10 diffusion pump used to pump the nozzle chamber. The nozzle is followed by two skimmers (Beam Dynamics), with 1.0 mm and 1.5 mm apertures, respectively, which serve to extract and collimate the beam. The second skimmer also forms the entrance aperture to the first hexapole. The two hexapoles which provide the A and B fields are identical. Each hexapole is 0.53 m long and constructed from six 1/4 in. centerless ground stainless steel rods mounted into perspex supports on an inscribed radius of 4.74 mm. An adjustable iris mounted into the connecting flange between the second hexapole and detection chambers forms the exit aperture for the second hexapole. For the experiments reported here this was set to a diameter of 2.5 mm. A thin stainless steel partition with a 9 mm diameter aperture separates the first hexapole chamber from the chamber housing the resonance cell, allowing the hexapole chamber to be pressurized during attenuation experiments and providing a known path length over which collisional attenuation of the beam can occur. There is a small amount of scattering gas leakage from the first hexapole chamber into the adjacent chamber, which houses the RF cell. However, the pressure in the second chamber never rises high enough during the course of an experiment to cause significant attenuation of the beam in this chamber, remaining always at least an order of magnitude lower than the pressure in the collision cell. For nitrogen as the scattering gas at a pressure of 1×10^{-5} Torr, the pressure in the resonance cell

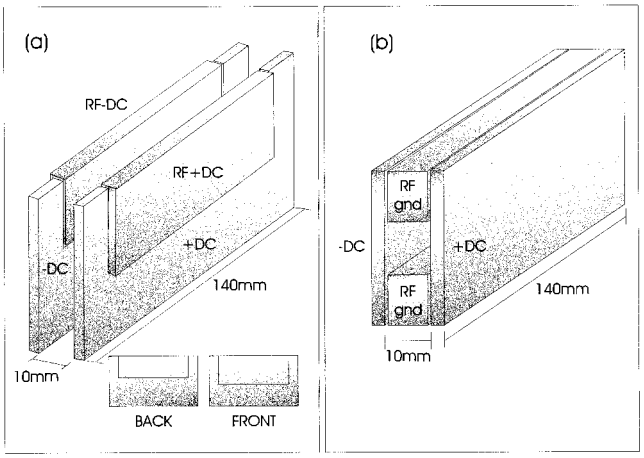

Figure 2. Split parallel plate (a) and double parallel plate (b) designs for the RF resonance cell.

rises by about 2×10^{-7} Torr. The resonance cell, positioned between the two hexapoles, is enclosed in a Faraday cage to prevent field penetration from the hexapoles into the C field region. Holes (10 mm) in each end of the mesh cage allow passage of the molecular beam. The beam signal is measured using an Extranuclear Laboratories 4-270-9 quadrupole mass spectrometer positioned at the focal point, 20 cm from the exit aperture of the second hexapole.

Two different geometries were tested for the resonance cell, both of which are shown in Figure 2. The first was based on the cell used by Wiediger et al.[9] and consists of a pair of split polished copper parallel plates across which a DC field is applied. Each plate is sectioned into two pieces in such a way that when an additional RF potential is applied to half of each plate a component of the oscillating field is present perpendicular to the DC field. The second design is more straightforward and consists of two pairs of polished copper parallel plates mounted at right angles to each other. A DC field is established between one pair of plates and RF is applied across the other. A comparison of spectra for the two resonance cells, Figure 3, shows that while the split plate cell gives superior resolution the second cell gives significantly higher signal amplitudes and is therefore more suitable for attenuation experiments. Four different electrical supply configurations were considered for the double parallel plate cell and scans over a single spectral line were collected under identical conditions in order to determine the optimum arrangement. As shown in Figure 3, arrangements iv and v gave comparable signal intensity and peak shape. Arrangement v was used in these experiments due to the relative simplicity of the electronic configuration required. The second design was found to give slightly better signals than the first, probably due to the more favorable relative orientations of the RF and DC electric field vectors.

In these experiments the RF frequency is held constant, and the DC field applied to the resonance cell is swept in order to record a spectrum. The DC potential is supplied by Spellman MSO.3N12/C and MSO.3P12/C computer controllable power supplies and is typically incremented in steps of 0.1 V or less. The RF is supplied by a Hewlett-Packard 33120A wave form generator. For optimum signal the frequency is fixed at between 1 and 3 MHz with an amplitude of around 1.0 V. Low RF amplitudes result in small signals due to low numbers of transitions being excited by the low intensity radiation, while high amplitudes lead to signal saturation, as shown in Figure 4. The RF amplitude is modulated by a square wave with a duty cycle of 0.5 and a frequency of typically around 500 Hz supplied by the function generator of a Goldstar OS-9020G oscilloscope. The modulating frequency is supplied as the reference to a Stanford Research Systems SR510 lock-in amplifier, and the modulated signal from the quadrupole mass spectrometer is supplied as the signal input. The amplitude of the modulation in the signal from the mass spectrometer is only a few percent of the total signal intensity. The RF modulation frequency is chosen so that the phase difference introduced by the flight time of the beam from the resonance cell, where the ΔM transitions are occurring, to the quadrupole mass spectrometer, where they are detected, is 360°, so that the phase on the lock-in amplifier can be set to zero. The correct frequency is determined by recording the lock-in signal as a function of modulating frequency and finding the frequency at which the signal is a maximum.

In order to measure a collision cross section the DC potential is tuned to the energy of the desired rotational state and the hexapole high voltage is set for transmission of the state. Gas is admitted to the first hexapole chamber through a Leybold Heraeus leak valve computer controlled using a Crystalap STD206 stepping motor. The pressure is usually incremented from around 4×10^{-6} to 3×10^{-5} Torr in steps of 1×10^{-6} Torr. The modulated signal detected by the lock-in amplifier is measured as a function of the scattering gas pressure and converted to a cross section using eq 6. The pressure in the collision cell is measured using a Model 690A high accuracy (0.15% of reading) 0.1 Torr MKS Baratron with Model 670 signal conditioner, to 1×10^{-5} Torr. An MKS Instruments Model 919 hot cathode controller coupled to a Duniway T-100-K ion gauge is calibrated against the Baratron from 0.1 to 1×10^{-5} Torr and extrapolated to 1×10^{-6} Torr for each scattering gas allowing absolute pressure measurements to be made over the range of interest. Pressure measurements using the 919 controller are reproducible to within ±5%. The absolute accuracy attainable for the cross section measurements is dominated by the uncertainty in the pressure measurements. This is estimated from instrument specifications to be 0.15% above 1×10^{-5} Torr and up to 5% for pressures below 1×10^{-5} Torr. In practice, the attenuation curves show no obvious difference where measurements overlap these ranges. The temperature is measured with a chromel−alumel thermocouple to an accuracy of better than 0.2% at 300 K, and the geometric length of the collision cell is known to an accuracy of 0.1%. During an experiment the pressure in the collision cell is varied over a range from 1 to 2 orders of magnitude higher than the pressure in the resonance cell. The increase in resonance cell pressure due to effusive transfer of gas through the 9 mm diameter hexapole aperture and the 10 mm diameter cell enclosure aperture will change the effective length of the collision cell by a millimeter or so. However, we observe no obvious curvature in the attenuation curves; even with the collision cell at the highest pressures, around 3×10^{-5} Torr, the pressure in the resonance cell is less than 1×10^{-6} Torr, and beam attenuation through collisions occurring in this region is small enough to be almost negligible. The uncertainty in the difference signal measurement determined with the lock-in amplifier is reflected in the reproducibility in the signal (Figure 6) and the standard deviation in the reported cross sections (Table 1). We consider the accuracy of the cross sections reported in this work to be better than 10% and more likely better than 5%.

4. Results and Discussion

All the experiments described in this work were carried out using a seeded beam of 10% CH_3F in argon. Initially, a

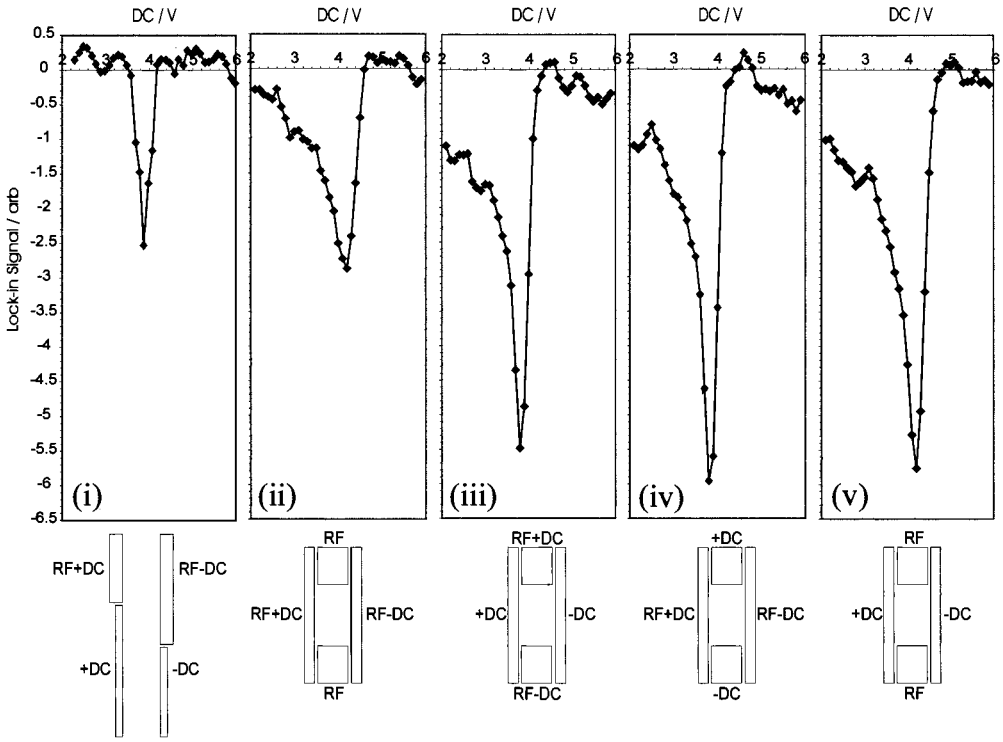

Figure 3. Scans of the |111⟩ peak using (i) the split parallel plate resonance cell and (ii−v) four different electrical supply configurations for the double parallel plate resonance cell. Scans were run at a hexapole voltage of 2000 V with an RF frequency of 2 MHz and RF amplitude 1 V.

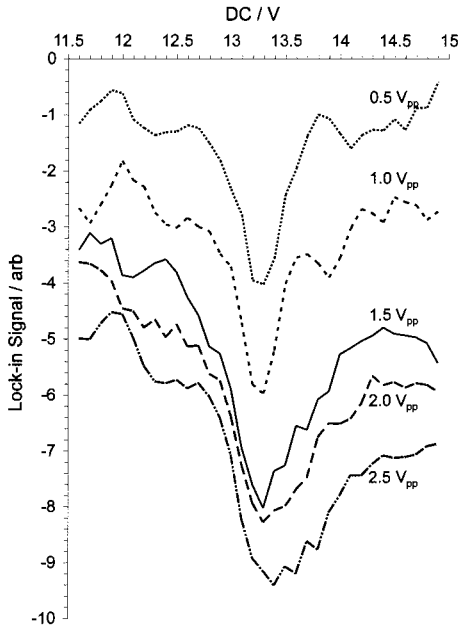

Figure 4. Effect of RF amplitude on the resonance signal measured for the |21⟩ peak of a 10% CH_3F/Ar beam at a hexapole voltage of 3000 V and RF frequency of 2 MHz.

resonance spectrum was measured in order to identify the rotational states present in the beam. This spectrum is shown in Figure 5, together with hexapole transmission curves for each major component of the beam.

Reasonable signal levels could be obtained for three rotational $|JK\rangle$ states; |11⟩, |21⟩, and |31⟩. Cross section measurements made at each of the maxima in the hexapole transmission curves showed an unexpected dependence of the measured cross section on the hexapole voltage, with cross sections measured at low hexapole voltages (<2000 V) tending to be significantly higher than those at higher voltages, often by around 15%. This effect

TABLE 1: Collisional attenuation cross sections for individual rotational states of a seeded beam of 10% CH_3F with a range of scatterers at a hexapole voltage of 5200 V

state	scatterer	σ/Å^2 (resonance method)	σ/Å^2 (hexapole collision cell[8])
|111⟩	He	246 ± 6	247
|111⟩	Ar	284 ± 10	270
|111⟩	Xe	317 ± 25	319
|111⟩	N_2	390 ± 21	390
|111⟩	CO_2	287 ± 16	
|111⟩	CH_4	376 ± 44	
|111⟩	CH_3F	654 ± 40	
|111⟩	SF_6	316 ± 19	
|211⟩	Ar	350 ± 24	
|311⟩	Ar	366 ± 17	

appears to be associated with the differing amplitudes of the fundamental, first-harmonic and second-harmonic trajectories of the symmetric top molecules through the hexapole at successively higher hexapole voltages. The presence of the resonance cell should have the smallest effect on the second-harmonic type trajectories, due to their lower maximum radial displacement and the fact that the molecules are traveling almost parallel to the axis when they enter the resonance cell. For this reason, all cross sections were measured at a hexapole voltage of 5200 V. This choice had the additional advantage that unlike the first or second harmonics, which appear at significantly different hexapole voltages for the various states, reasonable signal levels could be obtained for all three states at a single hexapole voltage. Five to ten repeated measurements were averaged to give the reported cross sections, shown in Table 1. A typical data set is shown in Figure 6.

The cross sections for collisional attenuation of the |111⟩, |211⟩, and |311⟩ states are seen to increase with increasing J, from 285 Å^2 for the |111⟩ state to 366 Å^2 for |311⟩. Although the difference between the cross section for the attenuation of the |111⟩ state is lower than the cross sections for the higher J states, which are the same within their respective uncertainties,

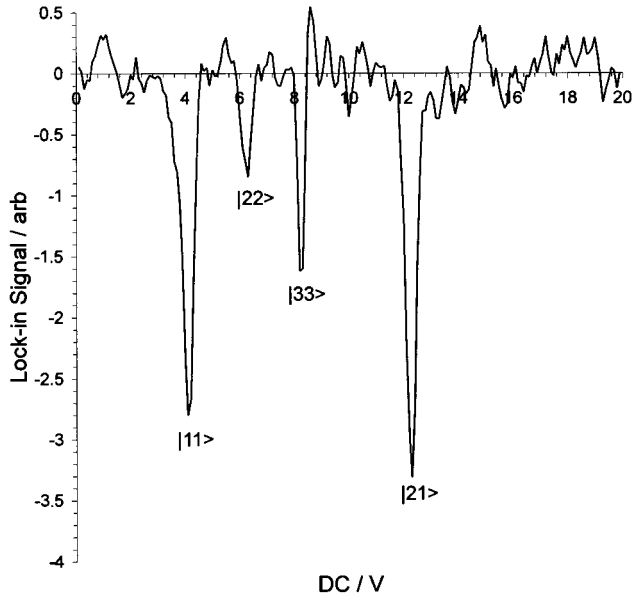

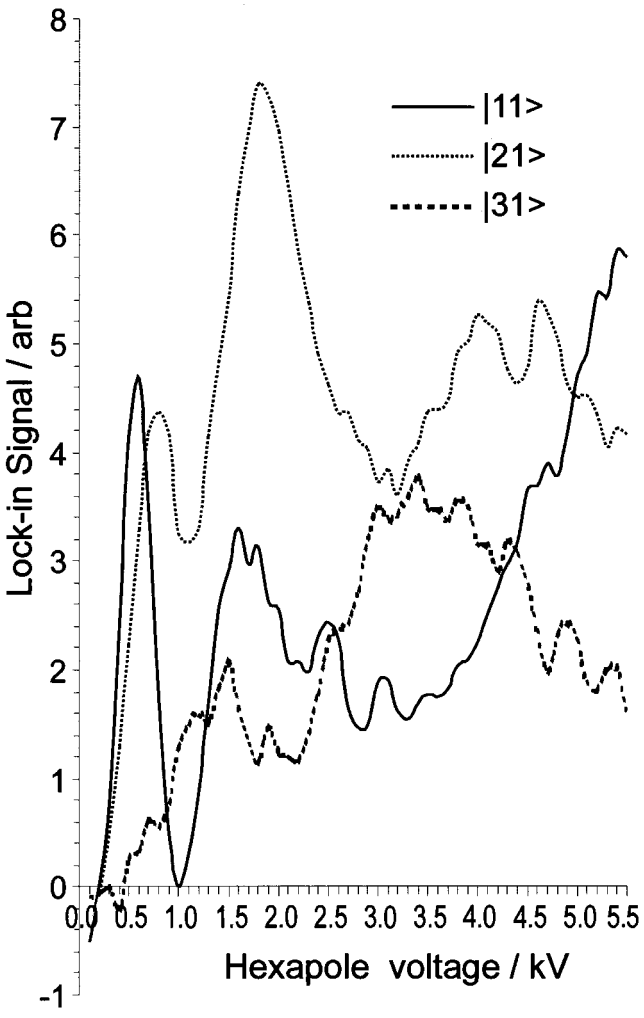

Figure 5. (a) Resonance spectrum of the rotational states present in a seeded beam of 10% CH_3F/Ar at a hexapole voltage of 4000 V, RF frequency 2 MHz, and amplitude 1 V. (b) Hexapole transmission curves for the $|111\rangle$, $|211\rangle$, and $|311\rangle$, rotational states.

the difference is not seen to be very significant. The energy associated with these transitions is <1 J mol^{-1} and the cross sections correspond to internuclear separations over the range from 9 to 11 Å.[7]

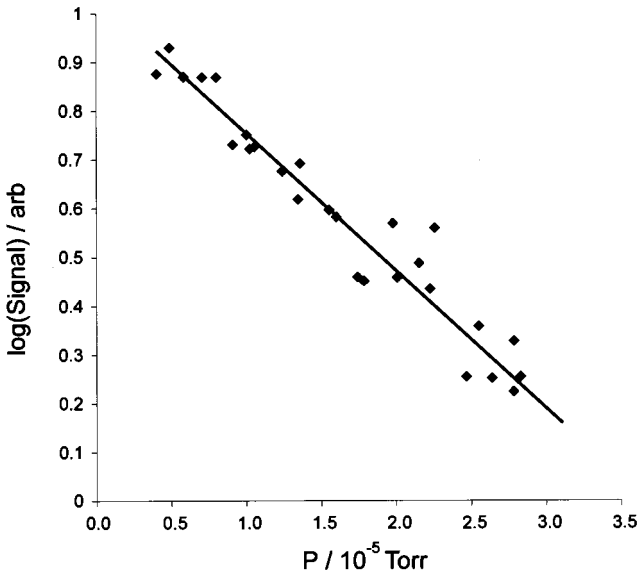

Figure 6. A typical data set used to determine the cross section for collisional attenuation of the $|111\rangle$ state of CH_3F by Ar at a hexapole voltage of 5200 V.

Attenuation cross sections for the $|111\rangle$ state were measured for a wide range of scattering gases. Data from the experiments of Blunt et al.[7,8] were available for the inert gases and nitrogen. In these experiments a single long hexapole collision cell replaced the double hexapole/resonance cell arrangement used in the work reported here. Hexapole transmission curves were measured as a function of scattering gas pressure in the hexapole and the collisional attenuation cross section for a given hexapole voltage was determined from the Beer−Lambert law as described in section 2.3. Cross sections for individual rotational states can in theory be obtained once the hexapole voltage at which they focus is known. However, in practice the resolution of the experiment is fairly low, and the signal at a given voltage will have contributions from several states other than the one of interest. It was only possible to extract cross sections for the $|11\rangle$ state with any degree of certainty. Despite these limitations, the cross sections measured using this technique are found to agree very well with those measured using the current method, in which the only contribution to the signal is from the rotational state to which the resonance cell is tuned. The excellent agreement between the two sets of data inspires confidence in the reliability of the resonance method for the measurement of collisional attenuation cross sections.

In addition to the measurement of cross sections for comparison with previous data, a series of measurements were made using SF_6, CH_4, CH_3F, and CO_2 as scattering gases. As expected, there is a general increase in the cross section with increasing molecular size and a large cross section for scattering from CH_3F. The uncertainty associated with this cross section is a little higher than for other scattering gases. The small amount of CH_3F leaking from the collision chamber into the resonance cell chamber makes its way into the chamber housing the quadrupole mass spectrometer giving a background level of CH_3F which is superimposed on the weak beam signal.

5. Conclusions

Measurements of ΔM changing collision cross sections for state-selected molecular beams of CH_3F seeded in Ar have shown that radiofrequency spectroscopy methods provide a powerful technique for determining the properties of individual

rotational states in a beam of symmetric top molecules. In the future the technique could be very useful for tagging individual states in crossed beam experiments. In addition, the ability to easily record a spectrum of the rotational states present in such a beam will facilitate the optimization of a particular state through control of the supersonic expansion, seeded beams, and selection of the hexapole voltage. We have shown previously[7] that the velocity dependence of these cross sections is consistent with a long range interaction based on dispersion and dipole-induced dipole contributions and that cross sections calculated assuming ΔM only transitions give values close to those measured.

Acknowledgment. We acknowledge the Marsden Fund for support of this project through Contract UOC605 which also provides a graduate fellowship for W-P. Hu and express our thanks to Phil Brooks for helpful suggestions and comments.

References and Notes

(1) Toennies, J. P. *Faraday Discuss. Chem. Soc.* **1962**, *33*, 96.
(2) Toennies, J. P. *Z. Phys.* **1965**, *182*, 257.
(3) Toennies, J. P. *Z. Phys.* **1966**, *193*, 76.
(4) Bennewitz, H. G.; Kramer, K. H.; Paul, W.; Toennies, J. P. *Z. Phys.* **1964**, *177*, 84.
(5) Borkenhagen, U.; Malthan, H.; Toennies, J. P. *Chem. Phys. Lett.* **1976**, *41*, 222.
(6) Borkenhagen, U.; Malthan, H.; Toennies, J. P. *J. Chem. Phys.* **1979**, *71*, 1722.
(7) Blunt, D. A.; Harris, S. A.; Hu, W. P.; Harland, P. W. *J. Phys. Chem. A* **1998**, *102*, 1482.
(8) Hu, W.-P.; Harris, S. A.; Harland, P. W.; Phillips, L. F. *Int. J. Quantum Chem.* **1998**. In press.
(9) Wiediger, S. D.; Harland, P. W.; Holt, J. R.; Brooks, P. R. *J. Phys. Chem. A* **1998**, *102*, 1112.
(10) Oka, T. *Adv. At. Mol. Phys.* **1973**, *9*, 127.
(11) Johns, J. M.; McKellar, A. R. W.; Oka, T.; Römheld, M. *J. Chem. Phys.* **1975**, *62*, 1488.
(12) Phillips, L. F. *J. Chem. Soc., Faraday Trans.* **1995**, *91*, 4363.